arXiv:astro-ph/0101375v2 14 Oct 2001

Could We Detect O_2 in the Atmosphere of a Transiting Extra-Solar Earth-Like Planet?

John K. Webb Imma Wormleaton

School of Physics, University of New South Wales, Sydney NSW 2052, Australia

Abstract

Although the extra-solar planets discovered so far are of the giant, gaseous type, the increased sensitivity of future surveys will result in the discovery of lower mass planets. The detection of O_2 in the atmosphere of a rocky extra-solar planet would be a potential indicator of life. In this paper we address the specific issue of whether we would be able to detect the O_2 A-band absorption feature in the atmosphere of a planet similar to the Earth, if it were in orbit around a nearby star. Our method is empirical, in that we use observations of the Earth's O_2 A-band, with a simple geometric modification for a transiting extra-solar planet, allowing for limb-darkening of the host star. We simulate the spectrum of the host star with the superposed O_2 A-band absorption of the transiting planet, assuming a spectral resolution of $\sim$8 km/s (typical of current echelle spectrographs), for a range of spectral signal-to-noise ratios. The main result is that in principle we may be able to detect the O_2 A-band of the transiting planet for host stars with radii $R \leq 0.3R_\odot$. However, using existing instrumentation and 8m telescopes, this requires target M stars with $m(V) \approx 10$ or brighter for integration times of ~ 10 hours or less. The number of such stars over the sky is small. Larger aperture telescopes and/or improved instrumentation efficiency would enable surveys of M stars down to $m(V) \approx 13$ and greatly improve the chances of discovering life elsewhere.

Keywords: stars:planetary systems

1 Introduction

In this paper we quantify the detectability of O_2 in the atmospheres of Earth-like planets in orbit around nearby stars. We investigate O_2 in particular because (a) it provides a potential indicator for forms of life which produce oxygen (Léger et al., 1994; 1999), (b) it produces a strong absorption band at optical wavelengths where high resolution spectroscopy can easily be done using large ground-based telescopes, and (c) the individual O_2 spectral lines are narrow, and the host star's peculiar velocity is likely to offset many of the extra-solar planetary O_2 lines from the telluric ones, enabling detection. Agreement between the observed velocity derived from the planetary O_2 lines, and the independently determined host star's peculiar velocity, would confirm the reality of the detection.

Low mass stars offer an easier target than larger stars for the detection of planetary transits, since a larger fraction of the stellar flux is blocked as the planet transits. However, for a planet orbiting in the habitable zone (HZ) of a low mass star, synchronous rotation may occur by about 4.5 Gyr after formation due to tidal damping (Kasting et al. 1993). However, Joshi et al. (1997) have produced detailed models of the atmospheres of terrestrial-type planets around M-stars. They conclude that, despite the synchronous rotator problem and possible stellar activity, planets orbiting M stars can support atmospheres over a large range of conditions and are very likely to be habitable.

Rosenqvist & Chassefière (1995) investigate upper limits for the O_2 partial pressure at a planetary surface for primitive abiotic atmosphere, finding an upper limit of ~ 10 mbar, compared to the terrestrial value of ~ 200 mbar. On this basis they suggest that the detection of large amounts of O_2 in the atmosphere of an extra-solar planet would be persuasive evidence for the presence of life.

A simple analytic estimate of the detectability of O_2 A-band has been carried out by Schneider (1994). He assumed a uniform stellar disk and an O_2 density which was constant with atmospheric height. No fine spectral details were considered since the calculation was based on the total equivalent width of the O_2 A-band feature. Here we extend Schneider's calculation with a more detailed investigation. The remainder of this paper is organised as follows: In Section 2, we use ground-based spectra to parameterise the Earth's atmospheric O_2 absorption. In Section 3 we apply that parameterisation to a transiting extra-solar planet. In Sections 4 to 6 we give quantitative estimates of the detectability of the O_2 A-band for various spectral signal-to-noise ratios and host stellar radii. We comment on the use of additional spectral features to improve the detection limits beyond those we report here. Finally, we summarise and discuss the simplifications made in our calculation.

2 Modelling the terrestrial O_2 A-band spectrum

To model the terrestrial O_2 A-band spectrum, we use high spectral resolution observations of the terrestrial O_2 A-band from two high redshift quasar spectra. The spectra of Q0019-1522 and Q0827+5255 were obtained using the Keck telescope with the HIRES spectrograph. Due to incomplete wavelength coverage in the Q0019-1522 spectrum, and high redshift absorption contamination in the spectrum of Q0827+5255, the two spectra were used to provide a complete, high resolution, uncontaminated spectrum. These spectra are ideal for the purpose, as their intrinsic spectra are otherwise featureless in the wavelength range of the O_2 A-band features.

Our aim is to explore detection sensitivity for the O_2 A-band absorption of an extra-solar Earth-like planet as it transits its host star. One of the variables we explore later is the spectral signal-to-noise ratio of the host star. To generate extra-solar simulations we thus start with a simply-parameterised, noise-free model of the terrestrial O_2 A-band absorption. We obtain this from an empirical fit to the individual absorption lines in the terrestrial A-band. From the observed spectrum, we selected the 28 strongest lines in the spectral range $7623 - 7699$Å, and fitted Voigt profiles to each one individually using VPFIT, a non-linear least-squares Gauss-Newton algorithm[1]. The fitting procedure provides an initial "relative column density", $\mathcal{N}_i$, for each of the 28 lines. The parameters required to generate one absorption line include column density, intrinsic line width, oscillator strength, absorption coefficient, and laboratory wavelength.

[1] http://www.ast.cam.ac.uk/∼rfc/vpfit.html

The absolute O_2 column density measured on Earth looking towards the zenith is

$$N(r) = \int_0^H \rho(r) dr \quad (1)$$

$$= \rho_\circ \int_0^H e^{-r/h} dr \quad (2)$$

The O_2 number density at the Earth's surface is $\rho_\circ = 5.3 \times 10^{24}$ particles m^{-3} and the O_2 scale height is $h = 7.7$ km (NASA website[2]), so for $H \to \infty$,

$$N_\oplus = h\rho_\circ \quad (3)$$

$$= 4.1 \times 10^{24} \quad \text{particles cm}^{-2} \quad (4)$$

This number applies to each of the 28 lines we fitted. The HITRAN database[3] (Rothman et al. 1998) lists (with relative line strengths) a total of 108 O_2 A-band features in the spectral range $7595 - 7707$Å. We plotted the 28 fitted $\mathcal{N}_i$ against the corresponding "line strength" parameter from the HITRAN database and found a very tight linear relationship over 2 orders of magnitude in column density. This enabled us to compute "relative column densities", $\mathcal{N}_i$, for all 108 lines in the HITRAN database, including multiply-blended, very weak lines, which would otherwise be difficult to fit.

The tight linear relationship described above shows that the 28 strongest O_2 lines correspond well to the linear part of a curve-of-growth, so that for an individual absorption line, the absorption equivalent width, W, obeys $W \propto N\zeta\lambda$. We can therefore produce a "relative oscillator strength", ζ_i, for each of the 108 lines,

$$\zeta_i = \mathcal{K}\frac{\mathcal{N}_i}{N_\oplus} \quad (5)$$

where for convenience, the proportionality constant $\mathcal{K}$ was chosen such that $\zeta_i = 1$ for the strongest O_2 line.

We thus end up with a table of 108 values for ζ_i (derived as above) and precise corresponding wavelengths (from the HITRAN database) which can then be used to generate a set of Voigt profiles giving a good fit to the entire observed O_2 A-band.

The advantage of this method is that we can model the O_2 A-band as seen in transmission against an extra-solar planet as it transits its host star using a *single* parameter, the geometrically re-scaled O_2 column density. The intrinsic line width, which we approximate as being the same for all O_2 lines, is derived directly from the terrestrial observations. A more detailed model would take into account the decreasing intrinsic line width towards increasing wavelength. The comparison in Fig. 1 nevertheless shows that the approximation is acceptable. The synthetic spectrum derived in this way is illustrated in Figure 1. It gives a good detailed fit to the observations and therefore to the total observed equivalent width across the O_2 A-band.

3 Modelling the O_2 A-band spectrum of a transiting extra-solar Earth-like planet

We make a number of simplifications for ease of calculation: (a) the planet occults the host star centrally, (b) the host star has a featureless spectrum, (c) telluric O_2 terrestrial absorption is

[2]http://nssdc.gsfc.nasa.gov/planetary/planetfact.html

[3]http://CfA-www.Harvard.edu/HITRAN

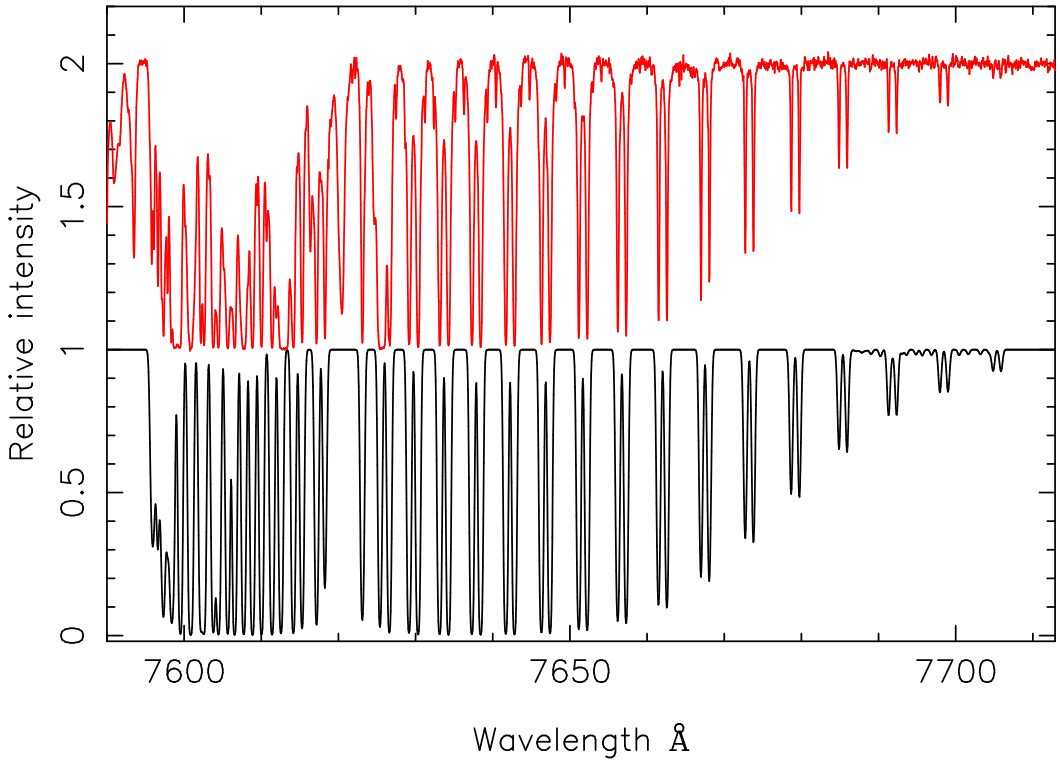

Figure 1: The lower spectrum is the synthetic spectrum of the terrestrial O_2 A-band obtained by fitting Voigt profiles to the 28 strongest observed spectral features and then deriving relative line strengths for all 108 O_2 A-band absorption lines listed in the HITRAN database. The spectral resolution (FWHM) is 7.7 km/s and the pixel size is 0.06Å. The upper spectrum illustrates one of the two real spectra (Q0827+5255) used to derive the model. The real data have been shifted to a continuum level of 2 for illustration. Additional absorption is seen in the real spectrum due to redshifted intervening gas clouds unassociated with the O_2 A-band. The second spectrum of the O_2 A-band, Q0019-1522, is uncontaminated in that region. Overall the model provides a good representation of the data, although fails to produce as much absorption as the real data between $\sim 7595 - 7620$Å. This may either be due to our approximation of a constant individual line width, or there being more lines present than listed in the HITRAN database (this requires further investigation).

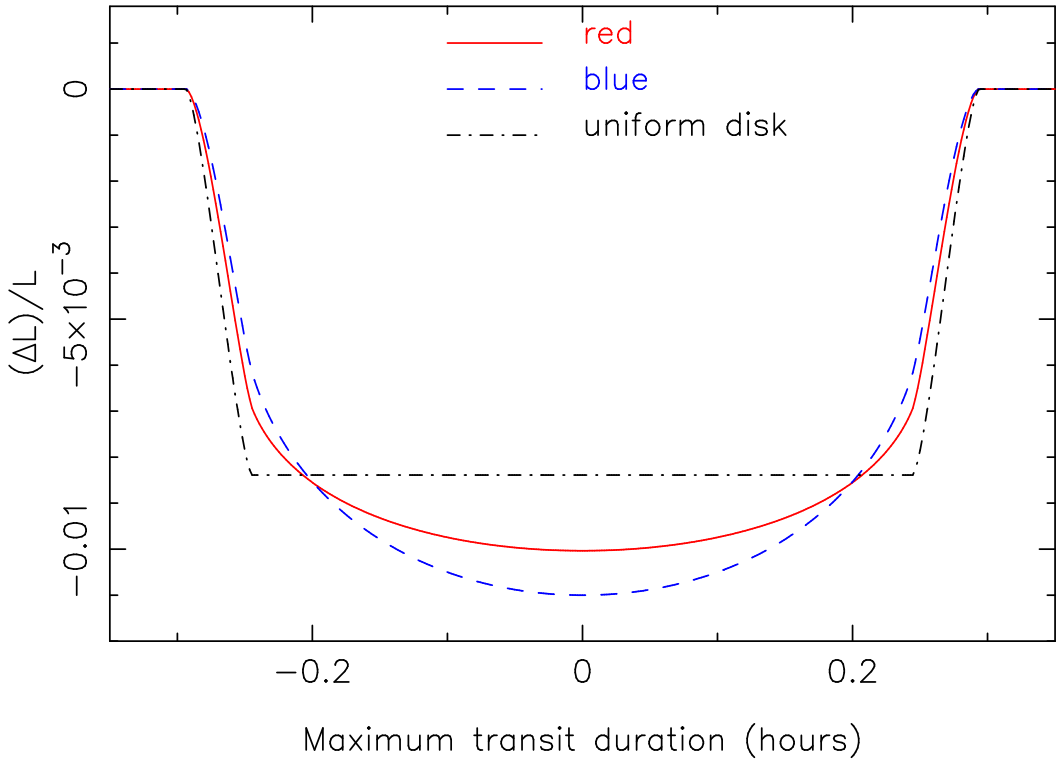

Figure 2: Simulated light curve for an Earth-size planet transiting a $0.1R_{\odot}$ star in an edge-on orbit. The 3 curves illustrate the wavelength dependent limb-darkening, using $u = 0.626$ and 0.394 for blue and red (Hestroffer & Magnan 1998). $(\Delta L)/L$ is the fractional luminosity change. The transit duration is given by equation 25, for $a = 0.03$ AU.

neglected, (d) refraction by the extra-solar planetary atmosphere is ignored. These simplifications are discussed in Section 6.3.

3.1 The residual starlight

Here we deal with the residual starlight which spills around the solid planet and its atmosphere, i.e. the light which is unaffected by either.

The stellar surface brightness decreases with projected radius. This limb-darkening effect is wavelength dependent (blue light is more centrally concentrated than red light) causing a wavelength dependent photometric light curve as the planet transits (Figure 2). Limb darkening also slightly favours the spectroscopic detection of the planet's O_2 A-band absorption. We parameterise the limb darkening effect by

$$I(\mu) = I_* \left[1 - u(1 - \mu)\right] \tag{6}$$

where I_* is the intensity at the centre of the stellar disk, u is a wavelength dependent limb-darkening coefficient. $u = 0.36$ at the O_2 A-band wavelengths (Hestroffer & Magnan 1998; Sacket 1999). μ is the cosine of the angle between the line of sight and the direction of the emerging flux, and is given by

$$\mu = \sqrt{1 - (x/R_*)^2} \tag{7}$$

where R_* is the stellar radius and x is the projected radius from the stellar centre.

The residual starlight is given by

$$F_{resid} = 2\pi \int_{R_H}^{R_*} I(\mu) x dx \tag{8}$$

where $R_H = R_p + H$, R_p is the planet radius and H is the maximum planetary atmosphere height (see Figure 3). We adopt $H = 100h$. Equation 8 integrates to give

$$\begin{aligned} F_{resid} &= \pi R_*^2 - \pi R_H^2 \left[1 - u - \frac{2u}{3} \left(1 - \frac{R_H^2}{R_*^2} \right)^{1/2} \right] & (9) \\ &\approx \pi R_*^2 - 0.4\pi R_H^2 & (10) \end{aligned}$$

for $u = 0.36$, where we have adopted a normalised stellar central intensity of $I_* = 1$.

3.2 The stellar flux transmitted through the planetary atmosphere

Figure 3 illustrates the geometry for a transiting planet. The O_2 column density along a line of sight grazing the extra-solar planet at an impact parameter x is

$$\begin{aligned} N(x) &= 2f \int \rho(r) dt & (11) \\ &= 2f\rho_\circ \int e^{-r/h} dt & (12) \end{aligned}$$

where the factor f is equal to unity for a terrestrial O_2 concentration. $h = \frac{kT}{mg}$ is the atmospheric scale height (7.7 km for O_2), k is Boltzmann's constant, T is a characteristic temperature, m is the mass of the species and g is the acceleration due to gravity for the planet (we neglect the height-dependence of g).

The path length along which we wish to integrate, t, depends on the height above the surface of the planet, r, the impact parameter x, and the Earth's radius, $R_p = 6,378$ km (NASA web site),

$$\begin{aligned} t &= \sqrt{(R_p + r)^2 - (R_p + x)^2} & (13) \\ dt &= \frac{(R_p + r) dr}{\sqrt{(R_p + r)^2 - (R_p + x)^2}} & (14) \end{aligned}$$

The column density at an impact parameter x therefore becomes

$$N(x) = 2f\rho_\circ \int_x^H \frac{e^{-r/h} (R_p + r) dr}{\sqrt{(R_p + r)^2 - (R_p + x)^2}} \tag{15}$$

The results are insensitive to the maximum atmospheric height out to which the integral is carried out, once $H \gg h$, due to the exponential density decline.

The spectrum associated with a particular impact parameter x, along a particular line-of-sight through the atmosphere, is then given by

$$I_\lambda(x) = I(\mu) e^{-\tau_\lambda(x)} \tag{16}$$

where $\tau_\lambda(x) = N(x) a_\lambda$ and a_λ is the (relative) absorption coefficient (chosen to correspond to the normalisation given in equation 5).

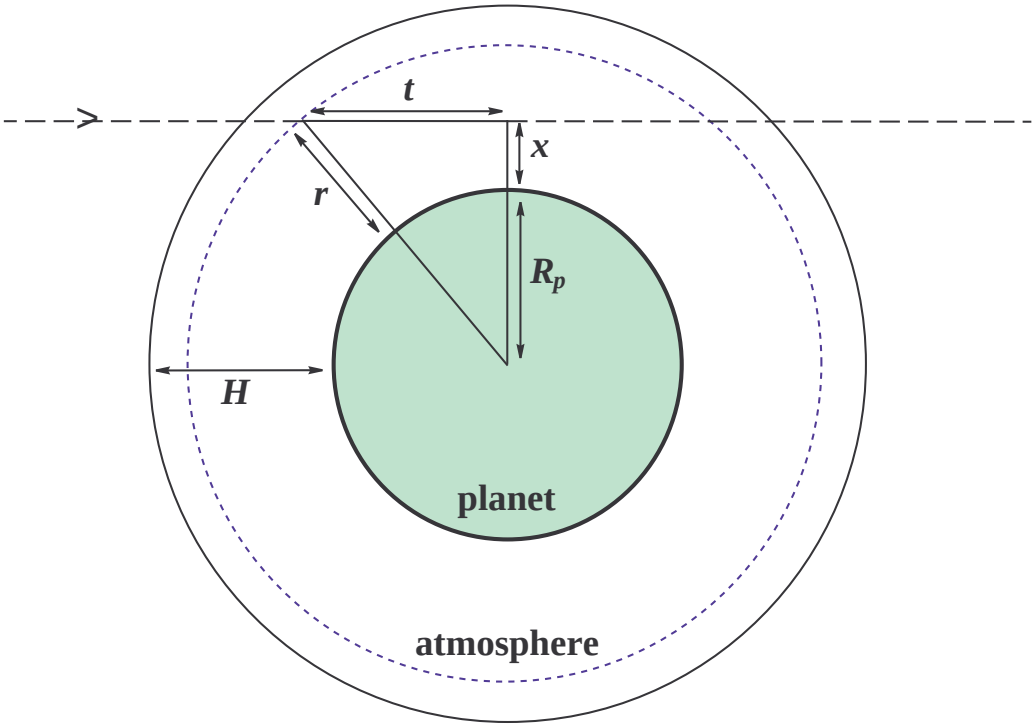

Figure 3: Geometry for extra-solar planet plus atmosphere. The line-of-sight through the atmosphere is horizontal in the plane of the diagram. R_p is the radius of the planet. r is the distance from the centre of the planet to a point within the atmosphere. The path length through the atmosphere, at an impact parameter x above the planet surface, is $2t$. H is the maximum atmospheric height considered. Absorption will occur over all possible path lengths through the sky-projected annulus.

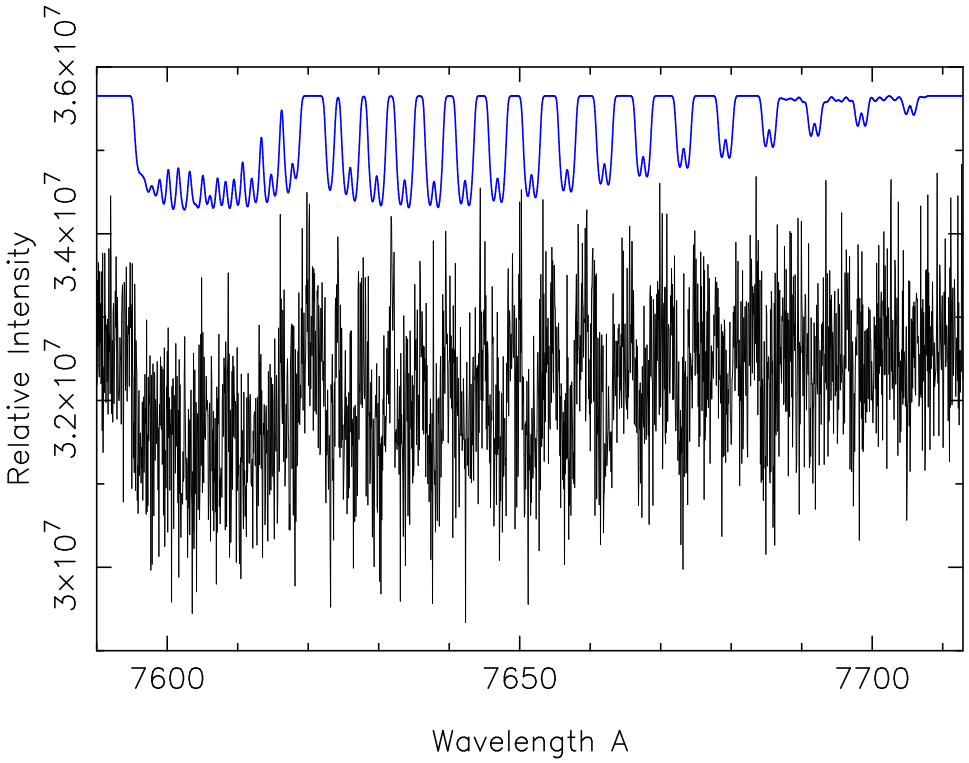

Figure 4: O_2 A-band theoretical spectrum of an Earth-like planet transiting a $0.1R_\odot$ star. The corresponding noise-free spectrum is shown, offset for illustration. The spectral signal-to-noise ratio is 18,000 per pixel, the spectral resolution (FWHM) is 7.7 km/s and the pixel size is 0.06Å. This is the most favourable case considered.

However, we need to allow for all possible lines of sight through the planetary atmosphere, so must integrate over the sky-projected annulus to obtain the observed spectrum due to starlight passing through the atmosphere,

$$F_{atmos} = 2\pi \int_0^H I_\lambda(x) x dx \tag{17}$$

which may be evaluated numerically.

3.3 The final spectrum

The flux observed from the host star is given by the sum of equations 10 and 17

$$F(\lambda)_{obs} = F(\lambda)_{atmos} + F_{resid} \tag{18}$$

where the λ dependence is shown to emphasise that, for simplicity, we approximate the underlying stellar light as a flat featureless continuum. The first term on the right hand of equation 18 is small and the O_2 A-band spectral signature of light transmitted by the planetary atmosphere is massively diluted by the residual starlight.

4 Measurement bounds

Using the results of Section 3, equation 18 enables us to generate synthetic spectra, $F(\lambda)_{obs}$, which we treat as "real data". The simulated spectrum is convolved with an instrumental profile

assumed to be Gaussian with FWHM = 7.7 km/s. We report the results for 4 stellar radii, $R_* = 0.1, 0.2, 0.3, 0.4 R_\odot$ ($R_\odot = 6.96 \times 10^5$ km) and 3 signal-to-noise ratios (per spectral pixel) of 6000, 12000, and 18000. These signal-to-noise ratios are attainable using existing high resolution echelle spectrographs on 8m-class ground-based telescopes. Integration times of several hours are required, for stellar magnitudes $m(V) \sim 5 - 10$, at the bright end of the M-star luminosity function.

We fit the "real data", with trial models, $G(\lambda, f)$. The concentration of O_2 in the extra-solar planetary atmosphere, as a fraction of the terrestrial value, f, is the only interesting free-parameter, assuming the stellar radius, R_*, is known from independent observations of the star. We used VPFIT to fit the n pixels over the spectral range $7590 - 7710$Å, computing

$$\chi^2 = \sum_{i=1}^{n} \frac{(F_i - G_i)^2}{\sigma_i^2} \tag{19}$$

where σ^2 is the variance per pixel in the "real data". To determine the error bounds on f, we use 3σ limits,

$$\Delta\chi^2 = (\chi^2 - \chi^2_{min}) \leq 9 \tag{20}$$

5 Results

One of the χ^2 curves is illustrated in Figure 5. The asymmetry of the χ^2 curve is to be expected, and was similar for all fits. Below $f = 1$, the observed absorption equivalent width is approximately proportional to column density. At higher values of f, the O_2 A-band begins to saturate, and a large increase in f then causes little change in the observed intensity. Thus, we are more sensitive to a lower limit than an upper limit.

Figure 6 illustrates the results for the range in parameter space we explored. 3σ bounds are plotted. Only at small R_* can both lower and upper limits be obtained, although lower limits are far more interesting. It appears feasible to obtain reliable detections of the O_2 A-band for combinations of $\{R_*;$ s/n$\}$ of $\{0.1 R_\odot;\ 6000\}$, $\{0.1, 0.2 R_\odot;\ 12000\}$, and $\{0.1, 0.2, 0.3 R_\odot;\ 18000\}$.

Our results seem to be less optimistic than those presented in tables 1 and 2 of Schneider (1994), who suggests that a 3-σ detection should be possible for an Earth-like planet seen against a host M-star, using a 2.4m telescope with an intergration time of 3.5×10^3 seconds). Specifically, the important result we find is that we should be able to detect the transmission absorption feature of the O_2 A-band in the atmosphere of an extra-solar planet as it transits a host star with $R_* \leq 0.3 R_\odot$, for s/n ≥ 12000.

6 Discussion

6.1 Transit time for a planet in the habitable zone

Repeated observations are possible (to build up spectral signal-to-noise) for the interesting case of a planet residing in the habitable zone (HZ) around a low mass host star. The maximum transit duration is (Sackett 1999),

$$t_T \quad = \quad \frac{P R_*}{\pi a} \tag{21}$$

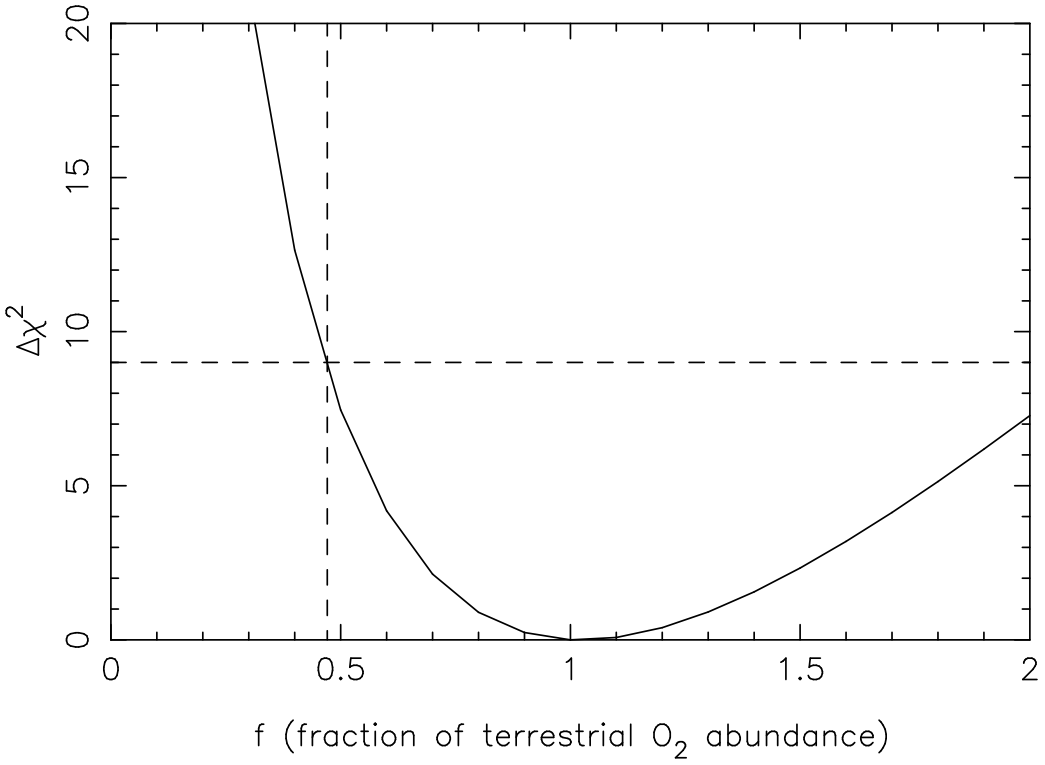

Figure 5: χ^2 minimisation to obtain the 3σ detection limits illustrated in Figure 6. This curve corresponds to the $\{R = 0.1R_p$; s/n=6000$\}$ point in Figure 6 (top left).

$$= \left(\frac{P}{675.4}\right)\left(\frac{R_*}{R_\odot}\right)\left(\frac{1\text{AU}}{a}\right) \tag{22}$$

$$\approx \left(\frac{P}{675.4}\right)\left(\frac{M_*}{M_\odot}\right)\left(\frac{1\text{AU}}{a}\right) \tag{23}$$

(e.g. Allen, 1999) and we can use Kepler's 3rd law

$$P = \left(\frac{a}{1\text{AU}}\right)^{3/2}\left(\frac{M_\odot}{M_*}\right)^{1/2} \text{ years} \tag{24}$$

to get the maximum transit time in hours,

$$t_T \approx 13\left(\frac{a}{1\text{AU}}\right)^{1/2}\left(\frac{M_*}{M_\odot}\right)^{1/2} \text{ hours} \tag{25}$$

Approximate values of the orbital radii for planets in the habitable zone are $a_{HZ} = 0.03$, 0.09, 0.15, 0.2 AU for stellar masses of 0.1, 0.2, 0.3, 0.4 $M_\odot$ (Kasting 1993). Using equation 25, the maximum transit times for planets in these orbits are 0.7, 1.7, 2.8, 3.7 hours. The corresponding orbital periods are 6, 22, 122, 163 days, so repeated high resolution spectral observations are feasible in order to build up a sufficient spectral signal-to-noise ratio.

6.2 The number of potential targets

Life-bearing planets are clearly the most interesting, so we consider the potential number of suitably bright M-stars, with Earth-like planets in their HZ's, and which are in edge-on orbits so

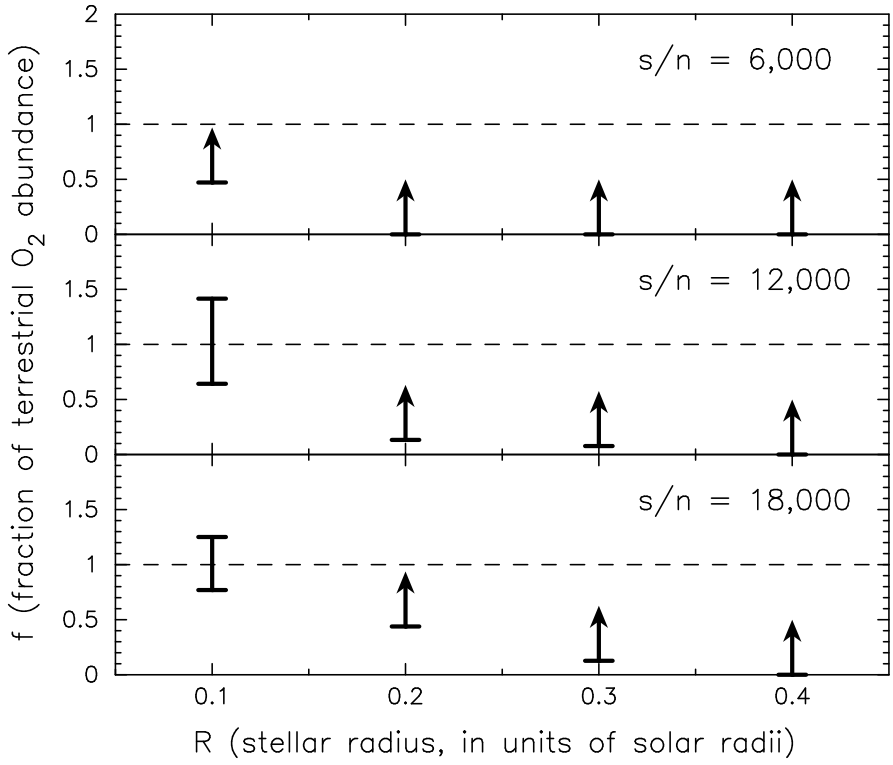

Figure 6: 3σ detectability bounds for O_2 A-band absorption in the atmosphere of a transiting planet with a terrestrial O_2 abundance. Each panel indicates the results of simulations of spectra with different signal-to-noise ratios. For the 2 cases where both upper and lower limits were possible, the bounds illustrated are $\pm 3\sigma$. The arrows indicate that the upper bounds are larger than $f = 2$. Significant detections are possible for $R \leq 0.3R_p$ when s/n ≥ 12000.

we could detect them. The number of potential targets is given by the product of the number of available M stars stars down to a given limiting magnitude, n_*, the fration of those stars which have an Earth-like planet in the HZ, $f_\oplus$, and the probability of there being an edge-on orbital alignment, i.e. the number of potential targets is

$$\mathcal{M} \approx \frac{n_* f_\oplus R_*}{a} \tag{26}$$

We assume a potential survey covers the whole-sky. There are approximately 80, 380, 1350, and 4800 M-stars down to limiting magnitudes of $m(V) = 10, 11, 12$ and 13. If the observations were carried out using existing echelle spectrographs on current ground-based 8m optical telescopes, our simulations suggest that an integration time of ~ 10 hours only reaches $m(V) = 10$. A larger telescope aperture or/and better overall telescope/instrumentation efficiency is required to achieve an improvement of, say, of a factor ~ 15 in the photon count-rate, to be able to carry out this experiment using observations of $m(V) = 13$ M-stars.

Wetherill (1996) investigates in detail the formation of planets around stars of various mass. His simulations produce the fascinating result that the probability of forming habitable planets is greatest at a planet-star separation of 1AU around a $1M_\odot$ star. Up to about 15% of $0.5M_\odot$ stars have habitable planets, although these generally have masses smaller than that of the Earth. The results are sensitive to the assumed initial surface density of planetesimals. To increase the planet yield, the surface density would need to be more centrally concentrated than that for the solar system. If we assume that a survey could be carried out for $m(V) = 13$ M stars, take $f_\oplus = 0.15$ and $R_* = 0.3R_\odot$, this rough calculation gives a total of 5 M stars, with habitable planets which are in edge-on orbits. Those targets would be pre-selected using photometric transit observations. A telescope which is considerably greater than 8m diameter would seem to be required to have a good statistical chance of detecting life elsewhere on an Earth-like planet by this technique.

6.3 Approximations and limitations

Finally, we summarise the simplifications used in the calculations described in this paper, discuss the limitations they lead to, and hence indicate some of the considerations for a real detection.

1. We did not compute an atmospheric model but instead found a simple way of parameterising the O_2 A-band absorption. Our results relate specifically to a transitting planet with the same atmosphere as our Earth. A more sophisticated calculation could be based on computing a model atmosphere and exploring detectability for a range of physical atmospheric parameters.

2. We did not allow for the telluric O_2 A-band. In practice the extra-solar planet O_2 A-band will be shifted with respect to the telluric lines, but only by $\lesssim 1/40$ of the width of the telluric band (for stellar peculiar velocities of $\lesssim 100$ km/s). The telluric and weak extra-solar planet O_2 A-band would therefore be confused. At wavelengths longwards of ~ 7620Å, there remains a reasonable amount of inter-line continuum against which some fraction of the offset extra-solar planet lines may be measured. Shortwards of ~ 7620Å, the increased line crowding will make detection harder. Note that the actual peculiar velocity of the host star will influence the detectability of the planet, depending on the degree of overlap between the planet and stellar O_2 lines. Variability of the telluric lines on time-scales shorter than the time-scale for a single on-target exposure will reduce the detectability. Further observational work is needed to investigate the details of this latter point before the effect can be properly included in an analysis like ours.

3. We made the approximation that the host star has a featureless spectrum. In practice, one would obviously have to attempt detection of the extra-solar planet atmosphere against a

complex background stellar spectrum. As with the telluric lines, any variability of the stellar spectral features on time-scales less than or comparable to a single on-target exposure will cause problems. Again, further observations are required to quantify this before it can be properly taken into consideration.

4. Our calculation was restricted to the static situation of the planet centrally obscuring the host star. In practice, the effect of the planet motion will complicate matters in several ways. For example, there will be a time-dependent asymmetry of the spectral features in the host star spectrum, as the planet obscures different velocities across the stellar surface. The asymmetry will also be wavelength dependent due to limb-darkening effects. The orientation of the planetary orbital plane with respect to our line-of-sight would need to be taken into consideration in the analysis of real data.

5. No attempt was made to include refraction of the stellar light by the atmosphere of the transitting planet. This may alter the absorption profile shapes. We assumed Voigt profiles. Refraction by the atmosphere of a transitting planet has recently been discussed by Hubbard et al. (2001).

6. Our calculations were based only on the O_2 A-band band. The detection sensitivity could be improved by simultaneously including other features such as the O_2 B-band, O_3, water vapour and methane. It is possible that detections could be made against larger stellar radii, if additional absorption features are incorporated into the analysis.

In the analysis of real data, considerations such as those above suggest that detection may best be attempted using differential spectroscopic methods, which would hopefully overcome any short-timescale variability problems. Complex modelling will still be required in order to interpret results. Models will need to be sophisticated compared to the simple calculation we have described in this paper. However, the results we report at least indicate that in principle it may be possible to detect oxygen in the atmosphere of a transitting extra-solar planet.

Acknowledgements

We are very grateful to Michael Ashley, Michael Box, Keith Horne, Charley Lineweaver, Gabriel Mititelu, Michael Murphy and Jill Rathborne for useful comments or discussions. We are also most grateful Bob Carswell, Sara Ellison and Jason Prochaska for providing the spectra with which we parameterised the terrestrial O_2 A-band.

References

Allen, C.W. 1999 in Allens Astrophysical Quantities, ed Cox, A.N., (New York: Springer-Veralag), p382

Hestroffer, D. & Magnan, C. 1998 A&A, 333, 338

Hubbard, W.B., Fortnet, J.J., Lunine, J.I., Burrows, A., Sudarsky, D., Pinto, P., 2001 astro-ph/0101024

Joshi, M.M., Haberle, R.M., Reynolds, R.T. 1997 Icarus 129, 450

Kasting, J.F., Whitmire, D.P., Reynolds, R.T 1993 Icarus, 101, 108

Léger, A., Pirre, M., Marceau, F.J., 1994 Astrophys. & Space Science, 212, 327

Léger, A., Ollivier, M., Altwegg, K., Woolf, N.J., 1999 Astron. Astrophys., 341, 304

Rosenqvist, J., Chassefière, E. 1995 Planet. & Space Sci., 43, 3

Rothman, L.S. et al, 1998 J. Quant. Spec. & Rad. Trans., 60, 665

Sackett, P.D. 1999 in *Planets Outside the Solar System: Theory and Observations*, ed Mariotti J.-M. & Alloin D., Nato Science Series vol. 532, (Dordrecht: Kluwer), p189-227
Seager, S. & Sasselov, D.D. 2000 astro-ph9912241
Schneider, J. 1994 Ap & SS, 212, 321
Wetherill, G.W., 1996 Icarus, 119, 219